Sixth-order compact finite difference method for solving KDV-Burger equation in the application of wave propagations

K. Aliyi Koroche* and H. Muleta Chemeda

Abstract

Sixth-order compact finite difference method is presented for solving the one-dimensional KdV-Burger equation. First, the given solution domain is discretized using a uniform discretization grid point in a spatial direction. Then, using the Taylor series expansion, we obtain a higher-order finite difference discretization of the KdV-Burger equation involving spatial variables and produce a system of nonlinear ordinary differential equations. Then, the obtained system of a differential equation is solved by using the fourth-order Runge–Kutta method. To validate the applicability of proposed techniques, four model examples are considered. The stability and convergent analysis of the present method is worked by using von Neumann stability analysis techniques by supporting the theoretical and mathematical statements in order to verify the accuracy of the present solution. The quality of the attending method has been shown in the sense of root mean square error L_2 and point-wise maximum absolute error L_∞. This is used to show, how the present method approximates the exact solution very well and how it is quite efficient and practically well suited for solving the KdV-Burger equation. Numerical results of considered examples are presented in terms of L_2 and L_∞ in tables. The graph of obtained present numerical and its exact solution are also presented in this paper. The present approximate numeric solvent in the table and graph shows that the numerical solutions are in good agreement with the exact solution of the given model problem. Hence the technique is reliable and capable for solving the one-dimensional KdV-Burger equation.

* Corresponding author

Received 18 September 2021; revised 16 December 2021; accepted 18 December 2021

Kedir Aliyi Koroche
Ambo University, College of Natural and Computational Sciences, Department of Mathematics, Ambo, Ethiopia. gmail: kediraliyi39@gmail,com

Hailu Muleta Chemeda
Jimma University College of Natural Sciences Department of Mathematics, Jimma, Ethiopia. gmail: mulatah@gmail.com

1 Introduction

Partial differential equations (PDEs) are the mathematical equations that are significant in modeling physical phenomena that occur in nature. Applications of PDEs can be found in physics, engineering, mathematics, and finance. Examples include modeling mechanical vibration, heat, sound vibration, elasticity, and fluid dynamics [4]. Some applications in real life phenomena appear as nonlinear fractional order of PDEs. The fractional nonlinear PDE describes a variety of important physical phenomena, acoustics, elector-chemistry, materials science, fluid dynamics[2], optics, and visco-elasticity [1]. The other type of nonlinear PDEs is also Korteweg-de Vries Burgers' equation. Korteweg-de Vries Burgers' equation is a model mathematical statement for a wide class of nonlinear wave models of fluid in an elastic tube, liquid with small bubbles and turbulence [21]. This Burgers-Korteweg-de Vries (Burgers-KdV) equation has wide applications in physics, engineering, and fluid mechanics. The Poincaré phase plane analysis reveals that the Burgers-KdV equation has neither nontrivial bell-profile travelling solitary waves nor periodic waves [9].

The Burgers-KdV equation is the simplest form of the wave equation containing the nonlinearity, in which dispersion and the dissipation term occur [9]. It arises from many physical contexts, for example, the propagation of glandular bores in shallow water [5, 18], the flow of liquids containing gas bubbles [13], the propagation of waves in an elastic tube filled with a viscous fluid [36], weakly nonlinear plasma waves with certain dissipate effects [13, 16], and the cascading down the process of turbulence. It is also widely used as a nonlinear governing model in the crystal lattice theory, the nonlinear circuit hypothesis, and atmospheric dynamics [10].

Travelling waves or solitons as solutions to the Korteweg-de Vries equation (KdV), which is a nonlinear partial differential of mathematical statement four-third-order, have been of interest already for 150 years [37]. The Kdv equation was discovered in 1895 by Korteweg and de Vries [23], but this equation was forgotten for a long time. So that, the KdV equation is widely recognized as a paradigm for the description of weakly nonlinear long waves in many branches of physics and engineering. It describes how waves evolve under the competing but comparable effects of weak nonlinearity and dynamic dispersion [37]. Random waves are an important subject of haphazard PDEs [11]. The nonlinear problems are solved easily and elegantly without

converting to linear form the problem by using the Adomian decomposition method [22]. A feature common to all the traditional methods is that they are using the transformations to reduce the equation into a more simple mathematical statement and then solve it. Unlike classical techniques, the nonlinear equations are solved easily and elegantly without transforming the equation by using the Adomian decomposition method [21]. This wonderful technique has many advantages over classical techniques [22]. Mainly, it avoids the process of converting linear form and perturbation to find solutions to a given nonlinear equation. It provides an efficient explicit solution with high accuracy, minimal calculation, and avoidance of physically unrealistic assumptions [21].

Many authors studied the exact and numerical solutions of the KdV equation. Wadati [34] first introduced and studied the stochastic KdV equations and gave the diffusion of solutions to the KdV equation under Gaussian noise. Xie firstly studied research on Wick-type stochastic KdV equation on white noise spaces and showed the auto-Backlund transformation and the exact white noise functional solutions in [16]. Furthermore, Chen and Xie [6, 8] and Xie [7, 38] worked on some Wick-type stochastic wave equations using the white noise analysis method. Recently, Ũgurlu and Kaya [14] gave the tanh function method, Wazzan [35] showed the modified tanh-coth techniques, and these methods have been applied to derive nonlinear transformations and exact solutions of nonlinear PDEs in mathematical physics [18]. In those driving analytical methods, there is time consumed and very tired because it requires long computational time. To save our time and obtain an accurate approximate solution of the KdV equation, we use numerical methods.

Different numeral techniques give accurate denotative solutions for the KdV equation. To obtain the numerical solution of the KdV equations, the same researcher was used the traditionally, mesh-dependent methods such as the finite-difference method, finite element techniques, and boundary elements method. However, these methods have a slow rate of convergence, instability, low accuracy, and difficulty of implementation in complex geometries [4]. Even though the accuracy of the aforementioned methods is promising, they require large memory and long computational time. Besides funding, the methods are not suitable for higher-dimensional and problems involving complex geometries. Hence, the treatment of mesh-size presents several difficulties that have to be addressed to ensure the accuracy of the solution, and efficiency of the method applied [4]. Indeed scientists in the field of computational mathematics have been trying to develop numerical techniques by using computers for further application of different model problems. From those techniques, higher-order difference schemes and differential quadrature methods are more powerful techniques.

In many application areas, such as aeroacoustics [26] and electromagnetic [29], the propagation of acoustic and magnetic force waves needs to be accurately simulated over very long periods of time and far distances. Especially, the nonlinear partial differential equation is derived that plays a role in a

normal form, that is, in the first approximation, it determines the behavior of all solutions for the original boundary value problem with initial conditions from a sufficiently small neighborhood of equilibrium [20]. Therefore, in order to reduce the accumulation of errors during this process, the numerical algorithm must be highly accurate. To accomplish this goal, high-order compact finite difference schemes have been developed for simulating the solution of applications to wave propagation like [31, 32] and surface water modeling [27, 28]. The investigation of numerical solutions for nonlinear partial differential equations plays an important role in mathematics, physics, and other applied science areas.

High-order finite difference schemes can be classified into two main categories: explicit schemes and Pade-type or compact schemes. These hardcore techniques compute the numerical derivatives directly at each grid by using large stencils, while compact schemes obtain all the numerical derivatives along a grid line using smaller stencils for solving linear and nonlinear systems of equations. Experience has shown that compact schemes are much more accurate than the corresponding explicit scheme of the same order. Hence motivating this performance of implicit (Pade-type) scheme, this paper aims to construct an efficient and accurate sixth-order compact finite difference numerical method for solving a one-dimensional KdV-Burger equation in the application of wave propagation.

Statement of the problem

Consider a homogeneous KdV-Burger equations considered in [24] given by

$$U_t + aUU_x + vU_{xxx} = 0, \qquad (x,t) \in (0,b) \times (0,T), \tag{1}$$

with initial and boundary conditions, respectively,

$$U(x,0) = U_0(x), \qquad 0 \le x \le b, \tag{2}$$

$$U(0,t) = U_o(t), U(b,t) = U_b(t), \qquad 0 \le x \le T, \tag{3}$$

where $U_o(t)$ are $U_b(t)$ are periodic smooth functions and $0 \leqslant T < \infty$. Now we define a mesh size h and $\triangle t$ as constant grid points. They are defined by drawing distant horizontal and vertical lines of distance "h" and "$\triangle t$", respectively, in "x" and "t" directions. These lines are called grid lines, and the point at which they interact is known as the mesh point. This fabric topology point that lies at end of the domains, is called the boundary point. Points that lie inside the region are called interior points. The goal is to find the approximate solution of "$U(x,t)$" at the interior mesh points and to investigate how it converges too. Thus to do this, first, we discretized the solution domain concerning spatial direction as

$$0 = x_0 < x_1 < x_2 < \cdots < x_M = b,$$

where $x_{j+1} = x_j + h$ and $j = 1(1)M$. Moreover, M is the maximum number of grid points in the x-direction. Thus, to accomplish our work, the present paper is organized as follows. Section 2 is a description of numerical methods. Sections 3 is stability, consistence, and convergence analysis. Section 4 is the results of numerical experiments. Sections 5 is the discussion, and Section 6 is the Conclusion.

2 Description of proposed numerical method

2.1 Spatial discretization

In the high-order compact finite difference methods, the spatial derivatives in the governing PDEs are not approximated directly by some finite differences. They are evaluated by some compact difference schemes. We assume that $U(x, t)$ is a sufficiently smooth function and has continuous higher-order partial derivative on its domain. For the sake of simplicity, let $U(x_j, t) = U_j$ and let $\dfrac{\partial^\rho U(x_j, t)}{\partial x^\rho} = \partial_x^\rho U_j$ in which $\rho \geq 1$, be ρth-order partial derivative of $U(x, t)$ concerning with spatial variable x. By using the Taylor series expansion, we have

$$U_{j+1} = U_j + h\partial U_j + \frac{h^2}{2!}\partial_x^2 U_j + \frac{h^3}{3!}\partial_x^3 U_j + \frac{h^4}{4!}\partial_x^4 U_j + \cdots , \tag{4}$$

$$U_{j-1} = U_j - h\partial u_j + \frac{h^2}{2!}\partial_x^2 U_j - \frac{h^3}{3!}\partial_x^3 U_j + \frac{h^4}{4!}\partial_x^4 U_j - \cdots , \tag{5}$$

$$U_{j+2} = U_j + 2h\partial U_j + \frac{4h^2}{2!}\partial_x^2 U_j + \frac{8h^3}{3!}\partial_x^3 U_j + \frac{16h^4}{4!}\partial_x^4 U_j + \cdots , \tag{6}$$

$$U_{j-2} = U_j - 2h\partial U_j + \frac{4h^2}{2!}\partial_x^2 U_i - \frac{8h^3}{3!}\partial_x^3 U_j + \frac{16h^4}{4!}\partial_x^4 U_j - \cdots . \tag{7}$$

Now subtracting (7) from (11), we obtain

$$\partial U_j = \frac{U_{j+1} - U_{j-1}}{2h} - \frac{h^2}{6}\partial_x^3 U_j - \frac{h^4}{120}\partial_x^5 U_j - \cdots . \tag{8}$$

Hence from (10), we obtain the second-order central finite difference equation for the first-order partial derivative of $U(x, t)$ concerning spatial variable x given by

$$\delta_{cx}^{(1)} U_j = \frac{U_{j+1} - U_{j-1}}{2h} + T_1, \tag{9}$$

where $T_1 = -\dfrac{h^2}{6}\partial_x^3 U_j = \dfrac{h^2}{6}\partial_x^3 U(x_j, t)$ is its local truncation error. Again subtracting (9) from (8), we obtain

$$\frac{8h^3}{3}\partial_x^3 U_j = U_{j+2} - U_{j-2} - 4h\partial U_j - \frac{32h^5}{120}\partial_x^5 U_j - \frac{128h^7}{5040}\partial_x^7 U_j - \cdots. \quad (10)$$

Now substituting (10) into (10), we obtain

$$\frac{8h^3}{3}\partial_x^3 U_j = U_{j+2} - U_{j-2} - 4h\left(\frac{U_{j+1} - U_{j-1}}{2h} - \frac{h^2}{6}\partial_x^3 U_j - \cdots\right) - \frac{32h^5}{120}\partial_x^5 U_j - \cdots.$$

Collecting like terms in the above difference equation, we obtain

$$\partial_x^3 U_j = \frac{U_{j+2} - 2(U_{j+1} - U_{j-1}) - U_{j-2}}{2h^3} - \frac{7h^2}{60}\partial_x^5 U_j - \frac{31h^4}{2520}\partial_x^7 U_j - \cdots. \quad (11)$$

Hence from (14), we obtain the second-order central finite difference equation for third-order partial derivative of $U(x, t)$ concerning spatial variable x, given by

$$\partial_x^3 U_j = \frac{U_{j+2} - 2(U_{j+1} - U_{j-1}) - U_{j-2}}{2h^3} + T_2, \quad (12)$$

where $T_2 = -\dfrac{7h^2}{60}\partial_x^5 U_j$ is their local truncation error. Again substituting (11) and (7) into (9), we obtain

$$\delta_{cx}^{(1)} U_j = \frac{\left(U_j + h\partial_x U_j + \dfrac{h^2}{2!}\partial_x^2 U_j + \dfrac{h^3}{3!}\partial_x^3 U_j + \cdots\right)}{2h}$$
$$- \frac{\left(U_j - h\partial U_j + \dfrac{h^2}{2!}\partial_x^2 U_j - \dfrac{h^3}{3!}\partial_x^3 U_j - \cdots\right)}{2h} + T_1,$$
$$\delta_{cx}^{(1)} U_j = \partial_x U_j + \frac{h^2}{6}\partial_x^3 U_j + \frac{h^4}{120}\partial_x^5 U_j + \frac{h^6}{5040}\partial_x^7 U_j + \frac{h^8}{362880}\partial_x^8 U_j + \cdots,$$
$$\delta_{cx}^{(1)} U_j = \partial_x U_j + \frac{h^2}{6}\partial_x^3 U_j + \frac{h^4}{120}\partial_x^5 U_j + T_3, \quad (13)$$

where $T_3 = \dfrac{h^6}{5040}\partial_x^7 U_j$ is their principal local traction error. Again substituting (11)-(9) into (15), we obtain

$$\delta_{cx}^{(2)} U_j = \frac{(U_j + 2h\partial_x U_j + \cdots) - 2\left((U_j + h\partial_x U_j + \cdots) - (U_j - h\partial U_j - \cdots)\right)}{2h^3}$$
$$- \frac{(U_j + h\partial_x U_j + \cdots)}{2h^3} + T_2$$

$$\delta_{cx}^{(2)}U_j = \partial_x^3 U_j + \frac{31h^2}{120}\partial_x^5 U_j + \frac{8h^4}{315}\partial_x^7 U_j + \frac{51h^6}{72576}\partial_x^9 U_j + \cdots .$$

Thus from this, we obtain the second-order difference equation given by

$$\delta_{cx}^{(2)}U_j = \partial_x^3 U_j + \frac{31h^2}{120}\partial_x^5 U_j + \frac{8h^4}{315}\partial_x^7 U_j + T_4, \tag{14}$$

where $T_4 = \dfrac{51h^6}{72576}\partial_x^9 U_j$ is its principal local truncation error. Now using (2) and applying the successive derivative on it in terms of spatial variable x, we obtain the fifth- and sixth-order central difference scheme, and they are given by

$$\partial_x^5 U_j = \delta_{cx}^{(3)}\left(\delta_{cx}^{(2)}U_j\right), \tag{15}$$

$$\partial_x^7 U_j = \delta_{cx}^{(3)}\left(\delta_{cx}^{(3)}\left(\delta_{cx}^{(1)}U_j\right)\right). \tag{16}$$

Now substituting (15) into (13), we obtain

$$\delta_{cx}^{(1)}U_j = \partial_x U_j + \frac{h^2}{6}\partial_x^3 U_j + \frac{h^4}{120}\delta_{cx}^{(3)}\left(\delta_{cx}^{(2)}U_j\right) + T_3,$$

$$\delta_{cx}^{(1)}U_j = \partial_x U_j + \frac{h^2}{6}\delta_{cx}^{(3)}U_j + \frac{h^4}{120}\delta_{cx}^{(3)}\left(\delta_{cx}^{(2)}U_j\right) + T_3,$$

$$\frac{\partial U_j}{\partial x} = \delta_{cx}^{(1)}U_j - \frac{h^2}{6}\delta_{cx}^{(3)}U_j - \frac{h^4}{120}\delta_{cx}^{(3)}\left(\delta_{cx}^{(2)}U_j\right) - T_3. \tag{17}$$

Again substituting (15) and (16) into (14), we obtain

$$\delta_{cx}^{(2)}U_j = \partial_x^3 U_j + \frac{31h^2}{120}\delta_{cx}^{(3)}\left(\delta_{cx}^{(2)}U_j\right) + \frac{8h^4}{315}\delta_{cx}^{(3)}\left(\delta_{cx}^{(3)}\left(\delta_{cx}^{(1)}U_j\right)\right) + T_4,$$

$$\partial_x^3 U_j = \delta_{cx}^{(2)}U_j - \frac{31h^2}{120}\delta_{cx}^{(3)}\left(\delta_{cx}^{(2)}U_j\right) - \frac{8h^4}{315}\delta_{cx}^{(3)}\left(\delta_{cx}^{(3)}\left(\delta_{cx}^{(1)}U_j\right)\right) - T_4. \tag{18}$$

Now substituting (17) and (18) into (2), we obtain semi-discretization of the given governing PDE and the obtained nonlinear system of ordinary differential equation (ODE) is

$$\frac{dU_j}{dt} + aU_j\left(\delta_{cx}^{(1)}U_j - \frac{h^2}{6}\delta_{cx}^{(3)}U_j - \frac{h^4}{120}\delta_{cx}^{(3)}\left(\delta_{cx}^{(2)}U_j\right) - T_3\right)$$
$$+ v\left(\delta_{cx}^{(2)}U_j - \frac{31h^2}{120}\delta_{cx}^{(3)}\left(\delta_{cx}^{(2)}U_j\right) - \frac{8h^4}{315}\delta_{cx}^{(3)}\left(\delta_{cx}^{(3)}\left(\delta_{cx}^{(1)}U_j\right)\right) - T_4\right) = 0.$$

This implies that

$$\frac{dU_j}{dt} = aU_j\left(\frac{h^2}{6}\delta_{cx}^{(3)}U_j + \frac{h^4}{120}\delta_{cx}^{(3)}\left(\delta_{cx}^{(2)}U_j\right) - \delta_{cx}^{(1)}U_j\right) \tag{19}$$

$$+ v \left(\frac{31h^2}{120} \delta_{cx}^{(3)} \left(\delta_{cx}^{(2)} U_j \right) + \frac{8h^4}{315} \delta_{cx}^{(3)} \left(\delta_{cx}^{(3)} \left(\delta_{cx}^{(1)} U_j \right) \right) - \delta_{cx}^{(2)} U_j \right) + T_j,$$

where $T_j = \left(\frac{aU_j}{5040} \partial_x^7 + \frac{51v}{72576} \partial_x^9 \right) h^6 U_j$ is the jth terms of principal local truncation errors with order of accuracy $\mathbf{O}\left(h^6\right)$. Hence by truncating this local truncation error, our proposed scheme is

$$\frac{dU_j}{dt} = aU_j \left(\frac{h^2}{6} \delta_{cx}^{(3)} U_j + \frac{h^4}{120} \delta_{cx}^{(3)} \left(\delta_{cx}^{(2)} U_j \right) - \delta_{cx}^{(1)} U_j \right)$$
$$+ v \left(\frac{31h^2}{20} \delta_{cx}^{(3)} \left(\delta_{cx}^{(2)} U_j \right) + \frac{16h^4}{105} \delta_{cx}^{(3)} \left(\delta_{cx}^{(3)} \left(\delta_{cx}^{(1)} U_j \right) \right) - 6\delta_{cx}^{(2)} U_j \right),$$

$$\frac{dU_j}{dt} = \frac{ah^2 U_j}{6} \left(\frac{U_{j+2} - 2U_{j+1} + 2U_{j-1} - U_{j-2}}{2h^3} \right)$$
$$+ \frac{vh^4}{120} \left(\frac{U_{j+3} - 4U_{j+2} + 5U_{j+1} - 5U_{j-1} + 4U_{j-2} - U_{j-3}}{2h^3} \right)$$
$$- a \left(\frac{U_{j+1} - U_{j-1}}{2h} \right)$$
$$+ v \frac{31h^4}{20} \left(\frac{U_{j+3} - 4U_{j+2} + 5U_{j+1} - 5U_{j-1} + 4U_{j-2} - U_{j-3}}{2h^3} \right)$$
$$- 6v \left(\frac{U_{j+2} - 2U_{j+1} + 2U_{j-1} - U_{j-2}}{2h^3} \right)$$
$$+ \frac{128vh^4}{840} \left(\frac{1}{8h^7} \left(U_{j+5} - 4U_{j+4} + 3U_{j+3} + 8U_{j+2} - 14U_{j+1} \right. \right.$$
$$\left. \left. + 14U_{j-1} - 4U_{j-2} - 3U_{j-3} + 4U_{j-4} - U_{j+5} \right) \right).$$

This implies that

$$\frac{dU_j}{dt} = \frac{aU_j}{480h} \left(U_{j+3} + 36U_{j+2} - 315U_{j+1} + 315U_{j-1} - 36U_{j-2} - U_{j-3} \right)$$
$$+ \frac{v}{6720h^3} \left(U_{j+5} - 4(U_{j+4} - U_{j-4}) + 2607(U_{j+3} - U_{j-3}) \right)$$
$$+ \left(-30568(U_{j+2} - U_{j-2}) + 53326(U_{j+1} - U_{j-1}) - U_{j-5} \right),$$

which implies that

$$\frac{dU_j}{dt} = \frac{3aU_j}{160h} \left(0.1(U_{j+3} - U_{j-3}) + 36(U_{j+2} - U_{j-2}) - 315(U_{j+1} - U_{j-1}) \right)$$
$$+ \frac{0.5v}{3360h^3} (U_{j+5} - U_{j+5})$$
$$- \frac{v}{3360h^3} \left(2(U_{j+4} - U_{j-4}) + 1303.5(U_{j+3} - U_{j-3}) \right)$$
$$- \frac{v}{3360h^3} \left(15284(U_{j+2} - U_{j-2}) + 26663(U_{j+1} - U_{j-1}) \right),$$
$$\tag{20}$$

where $j = 0, 1, 2, 3, \ldots, M-1$. From (20), the nonlinear system of the ODE is given in the form of

$$\frac{dU_0}{dt} = \frac{3aU_0}{160h}\left(0.1(U_3 - U_{-3}) + 36(U_2 - U_{-2}) - 315(U_1 - 315U_{-1})\right)$$
$$+ \frac{0.5v}{3360h^3}(U_5 - U_{-5})$$
$$- \frac{v}{3360h^3}(2(U_4 - U_{-4}) + 1303.5(U_3 - U_{-3}) - 15284(U_2 - U_{-2})$$
$$+ 26663(U_1 - U_{-1}))$$

$$\frac{dU_1}{dt} = \frac{3aU_1}{160h}\left(0.1(U_4 - U_{-2}) + 36(U_3 - U_{-1}) - 315(U_2 - 315U_{-0})\right)$$
$$+ \frac{0.5v}{3360h^3}(U_6 - U_{-4})$$
$$- \frac{v}{3360h^3}(2(U_5 - U_{-3}) + 1303.5(U_4 - U_{-2}) - 15284(U_3 - U_{-1})$$
$$+ 26663(U_1 - U_{-0}))$$

$$\vdots$$

$$\frac{dU_{M-1}}{dt} = \frac{3aU_{M-1}}{160h}(0.1(U_{M+4} - U_{M-6}) + 36(U_{M+3} - U_{M-1})$$
$$- 315(U_{M+2} - 315U_M))$$
$$+ \frac{0.5v}{3360h^3}(U_{M+6} - U_{M-4})$$
$$- \frac{1}{3360h^3}\left(2(U_{M+5} - U_{M-3}) + 1303.5(U_M + 4 - U_{M-2})\right)$$
$$+ \frac{1}{3360h^3}\left(15284(U_{M+3} - U_{M-1}) - 26663(U_{M+1} - U_M)\right). \quad (21)$$

Now by introducing the vectors $U(t) = [U_1(t), U_2(t), U_3(t), \ldots, U_M(t)]^t$ in (21), we can rewrite the system of equation in the matrix form given by

$$\frac{dU(t)}{dt} = AH\left(U(t)\right) \quad (22)$$

subject to discretized initial and nondiscretized boundary conditions given by

$$U(x_j, 0) = U_0(x_j), \qquad 0 \le x_j \le b,$$
$$U(0, t) = U_0(t), \quad U(b, 0) = U_b(t), \qquad 0 \le t \le T, \quad (23)$$

and where H is a nonlinear function of U which contains the entries h_j give by $H(U_j) = h_j(U_1, U_2, \ldots, U_{M-1})$.

2.2 Temporary discretization

Consider the discretization of time domain $[0, T]$ by using the equidistant mesh-size with time step $\triangle t$ given as

$$D_n = \{t_{n+1} = t_n + \triangle t\}, \tag{24}$$

where $\triangle t = T/N$ and $n = 1(1)N$, in which N is the Maximum number of grid points in temporary (time) direction. Then the resulting system of Odes in (22) can now be solved by using the classical fourth-order Runge–Kutta method. This Runge–Kutta techniques integrate the value of U from n to $n + 1$ by using the operator given by

$$U_0 = U(x_j, t_0), \qquad K_1 = \triangle t A H(U_0),$$

$$U_1 = U_0 + 1/2 K_0, \qquad K_2 = \triangle t A H(U_1),$$

$$U_2 = U_0 + 1/2 K_1, \qquad K_3 = \triangle t A H(U_2),$$

$$U_3 = U_0 + 1/2 K_2, \qquad K_4 = \triangle t A H(U_2),$$

$$U_{n+1} = U_n + 1/6 \left(K_1 + 2K_2 + 2K_3 + K_4\right), \tag{25}$$

with both discretized initial and boundary conditions given by

$$U(x_j, 0) = U_0(x_j), \qquad 0 \leq x_j \leq b,$$

$$U(0, t_n) = U_0(t_n), \quad U(b, 0) = U_b(t_n), \qquad 0 \leq t_n \leq T,$$

where $j = 1(1)M - 1$ and $n = 1(1)N - 1$.

3 Stability, consistency, and convergence method

3.1 Stability of scheme

The stability of the proposed numerical method is investigated by using von Neumann stability analysis. To do this, we assume that the nonlinear term UU_x of partial differential equation in (2) as linear by taking $\gamma = U_j$, where γ is constant. Then without loss of generality, we obtain the linear system of ODEs. Assume that $\gamma = \max_j(U_j)$ in (20), and we can inquire about the eigenvalues of the M by M system of ODEs in (20). To obtain this eigenvalue, as [3, 12, 22, 25] takes, we assume that a trial solution is

$$U(x, t) = \varphi(t)\phi(x). \tag{26}$$

Furthermore to investigate the stability of the proposed method by von Neumann techniques, we assume that the trial function is defined by

$$\phi(x) = e^{iK_P x_j} = e^{ijhK_P}, \tag{27}$$

where $i = \sqrt{-1}$ and $K_P = P\pi$, $P = 1, 2, 3, \ldots, M$. Moreover, K is a Fourier number or amplification factor. Now substituting (26) and (27) into (20), we obtain

$$\frac{d\varphi(t)e^{ijhK_P}}{dt}$$
$$= \frac{3a\gamma\varphi(t)}{160h} \left(0.1(e^{ihK_p(j+3)} - e^{ihK_P(j-3)}) + 4(e^{ihk_P(j+2)} - e^{ihK_P(j-2)}) \right)$$
$$- \frac{3a\gamma\varphi(t)}{160h} \left(15(e^{ihK_P(j+1)} - e^{ihK_P(j-1)}) \right)$$
$$+ \frac{0.5v}{3360h^3} (e^{ihK_p(j+5)} - e^{ihK_p(j-5)})$$
$$- \frac{v\varphi(t)}{3360h^3} \left(2(e^{ihK_p(j+4)} - e^{ihK_p(j-4)}) + 1303.5(e^{ihK_p(j+3)} - e^{ihK_p(j-3)}) \right)$$
$$- \frac{v\varphi(t)}{3360h^3} \left(15284(e^{ihK_p(j+2)} - e^{ihk_p(j-2)}) + 26663(e^{ihk_p(j+1)} - e^{ihk_p(j-1)}) \right).$$

Dividing both sides by e^{ijhk_p}, this implies that

$$\frac{d\varphi(t)}{dt} = \frac{3a\gamma\varphi(t)}{160h} \left(0.1(e^{3ihK_p} - e^{-3ihK_p}) + 4(e^{2ihK_p} - e^{-2ihK_p}) \right)$$
$$- \frac{3a\gamma\varphi(t)}{160h} \left(15(e^{ihK_p} - e^{-ihK_p}) \right) + \frac{0.5v}{3360h^3}(e^{5ihK_p} - e^{-5ihK_p})$$
$$- \frac{v\varphi(t)}{3360h^3} \left(2(e^{4ihK_p} - e^{-4ihK_a}) + 1303.5(e^{3ihK_p} - e^{-3ihK_p}) \right)$$
$$- \frac{v\varphi(t)}{3360h^3} \left(15284(e^{2ihK_p} - e^{-2ihK_p}) + 26663(e^{ihK_p} - e^{-ihK_p}) \right) \tag{28}$$

Since for any differentiable function $\varphi(t)$, the Eigen-value problem of $\varphi(t)$ is

$$d\varphi(t)/dt = \lambda_p \varphi(t)$$

for $p = 1(1)M$. Hence substituting this into (28), we obtain

$$\lambda_p \varphi(t) = \frac{3a\gamma\varphi(t)}{160h} \left(0.1(e^{3ihK_p} - e^{-3ihK_p}) + 4(e^{2ihK_p} - e^{-2ihK_p}) \right)$$
$$- \frac{3a\gamma\varphi(t)}{160h} \left(15(e^{ihK_p} - e^{-ihK_p}) \right)$$
$$+ \frac{0.5v}{3360h^3}(e^{5ihK_p} - e^{-5ihK_p})$$
$$- \frac{v\varphi(t)}{3360h^3} \left(2(e^{4ihK_p} - e^{-4ihK_p}) + 1303.5(e^{3ihK_p} - e^{-3ihK_p}) \right)$$
$$- \frac{v\varphi(t)}{3360h^3} \left(15284(e^{2ihK_p} - e^{-2ihK_p}) + 26663(e^{ihK_p} - e^{-ihK_p}) \right).$$

Therefore this implies that

$$
\begin{aligned}
\lambda_p =& \frac{3a\gamma\varphi(t)}{160h} \left(0.1(e^{3ihK_p} - e^{-3ihK_p}) + 4(e^{2ihK_p} - e^{-2ihK_p})\right) \\
&- \frac{3a\gamma}{160h} \left(15(e^{ihK_p} - e^{-ihK_p})\right) + \frac{0.5v}{3360h^3}(e^{5ihK_p} - e^{-5ihK_p}) \\
&- \frac{v}{3360h^3} \left(2(e^{4ihK_p} - e^{-4ihK_a}) + 1303.5(e^{3ihK_p} - e^{-3ihK_p})\right) \\
&- \frac{v}{3360h^3} \left(15284(e^{2ihK_p} - e^{-2ihK_p}) + 26663(e^{ihK_p} - e^{-ihK_p})\right). \tag{29}
\end{aligned}
$$

From (29), using the Euler expiration into trigonometric form, we obtain

$$
\begin{aligned}
\lambda_p =& \frac{ia}{1680h^3} \left(0.5\sin(5hK_p) - 2\sin(4hK_p) + (6.3\gamma h^2 + 1303.5)\sin(3hK_p)\right) \\
&+ \frac{iv}{1680h^3} \left((252\gamma h^2 - 15284)\sin(2hK_p) + (945\gamma h^2 - 26663)\sin(hK_p)\right).
\end{aligned}
\tag{30}
$$

Hence from (30), we obtain the required Eigen-value. Real part of all Eigen-values is zero. This shows that strictly $Real(\lambda_p) \leq 0$ and so that, we have $|\lambda_p| < 1$ for all values of variable "p". Thus the required condition is satisfied. Therefore the obtained system of equation in (20) is stable.

Theorem 1. The difference mathematical statement given in (20) is stabilized equation if and only if all eigenvalues of coefficient matrix of obtained system of difference equation are simultaneously satisfy condition $Real(\lambda_a) \leq 0$.

Proof. The proof of this theorem is briefly given in [22].   □

3.2 Consistency of the scheme

Round-off errors and truncation errors occur when mathematical equations are solved numerically. Rounding errors originate from the fact that computers can only represent numbers (approximate solution) by using a fixed and limited number of significant figures. Therefore, such numbers cannot be represented exactly in different computer memories. The error introduced by this limitation is called a round-off error. Truncation errors in numerical investigation arise when approximations are used to estimate by using the finite term for infinite quantity by truncating certain terms from the boundless series term. Note that in numerical computation, if we work to minimize round-off error, then the truncation error is increased. Therefore it is difficult to avoid these errors in numerical computation. So that, in our work, we must find the balancing (equilibrium) points and minimize both of them simultaneously.

Generally, in all proposed numerical difference schemes, the accuracy of solution for a given mathematical problem obtained by those methods de-

pends on how small we make the step size, h, and time step $\triangle t$. Therefore, if the local truncation error produced in a numerical scheme is near to zero for which both h and $\triangle t$ simultaneously approach to zero, then this numerical method is called consistent.

Hence we have in-minding this, from our present proposed scheme in (20), that the principal part of local truncation error (the derived local shortening error) is

$$\lim_{j\to\infty} T_j = \lim_{j\to\infty} \left(\frac{U_j}{5040}\partial_x^7 + \frac{51}{12096}\partial_x^9 \right) h^6 U_j = 0.$$

Therefore from the above equation and the proposed theoretical-bounds of truncation error, we have $\max_j \|T_j\| \leq \mathbf{O}\ (h^6)$. Hence this implies that $\max_j \|T_j\| \longrightarrow 0$ as $h \mapsto 0$. So that, our scheme is consistent with the order of accuracy $\mathbf{O}\ (h^6)$.

3.3 Convergence analysis

Stability plus consistency of the proposed scheme leads to the convergence of the method. Hence our present system is both consistent and stable. So that, the outline present method is convergent with six-order of convergence in the spatial direction. To test the performance of this convergent and accuracy of the proposed method, we use the maximum point-wise absolute error, L_2 and L_∞ norms. Theses norms are calculated by

$L_\infty = \max_j |U(x_j,t_n) - U_{j,n}|$ and $L_2 = \sqrt{1/M \sum_{j=0}^M |U(x_j,t_n) - U_{j,n}|}$,

where M is the maximum number of grid points, $U(t_j,t_n)$ is exact and $U_{j,n}$ is an approximation solution of the KdV-Burger equation in (2) at the grid point (x_j,t_n). If the exact solution of the model problem does not exist, then we take the approximate solution $U_{2j,2n} \cong U(x_j,t_n)$ obtained at (x_j,t_n) by taking double number of grid-point as an exact result, and we can compare the error between them at specified grid points.

4 Results of numerical experiments

To test the validity of proposed method, we have considered the following model problem.

Example 1. Consider that one-dimensional KdV equation given by

$$U_t + \alpha \left(U^2 \right)_x + \beta U_{xxx} = 0$$

with periodic boundary conditions and the following initial condition:

$$(A)\quad U_0(x) = 3\ a\ \mathrm{sech}(G(x-c)) + 3\ b\ \mathrm{sech}^2(P(x-d))$$

$$a = 0.3, \ b = 0.1, \ c = 0.5, \ 0 \le x \le 2, \ 0 \le t \le 4,$$

$$\beta = 5.84 \times 10^{-4}, \alpha = 0.5, G = \alpha\sqrt{a/\beta}, P = \alpha\sqrt{b/\beta},$$

$$(B) \quad U_0(x) = 3 \ a \ \text{sech}(G(x - c)),$$

$$a = 0.3, \ c = 0.5, \ 0 \le x \le 1, \ 0 \le t \le 4,$$

$$\beta = 10^{-4}, \ G = 1/2\sqrt{a/\beta},$$

$$(C) \quad U_0(x) = \frac{2}{3} \ a \ \text{sech}^2(\frac{(x-1)}{\sqrt{108\beta}}),$$

$$a = 0.5, \ 0 \le x \le 3, 0 \le t \le 4,$$

$$\beta = 10^{-4},$$

Example 2. Consider the one-dimensional KdV equation considered in [37] given by

$$U_t + 6UU_x + U_{xxx} = 0.$$

With analytical solution obtained in [37] given by

$$U(x,t) = \frac{c}{2} \ \text{sech}^2(\frac{\sqrt{c}}{2}(x - ct - D)),$$

where D is a constant of integration.

Example 3. Consider the KdV equation considered in [30] given by

$$U_t + (\alpha + \beta U)UU_x + \gamma U_{xx} - \delta U_{xxx} = 0,$$

where initial condition of this equation for $\gamma = 0$ and $\delta = -1$ is given by

$$U(x,0) = -\frac{\alpha}{\beta}\left(1 + \tanh\left(\frac{\alpha}{2\sqrt{-6\beta}}x\right)\right).$$

In [30], by letting $\beta = 0$, $\alpha = 2$, $\gamma = -5$, and $\delta = -3$, its analytical solution is given by

$$U(x,t) = \frac{1}{3}\left(\text{sech}^2(\frac{\theta}{2}) + 2\tanh(\frac{\theta}{2}) + 2\right),$$

where $\theta = -\frac{1}{3}x + \frac{2}{3}t$.

Example 4. Consider that fractional KdV equation considered in [1] given by

$$\frac{\partial^\alpha U}{\partial t^\alpha} + U\frac{\partial U}{\partial x} + \frac{\partial^3 U}{\partial x^3} = F(x,t), \qquad (x,t) \in (0,1).$$

Analytical solution obtained in [1] is given by

$$U(x,t) = te^x,$$

by assuming $\alpha = 0.9$.

Table 1: Point-wise absolute error and root mean square error, for Example 1 (A) if $M = 61$

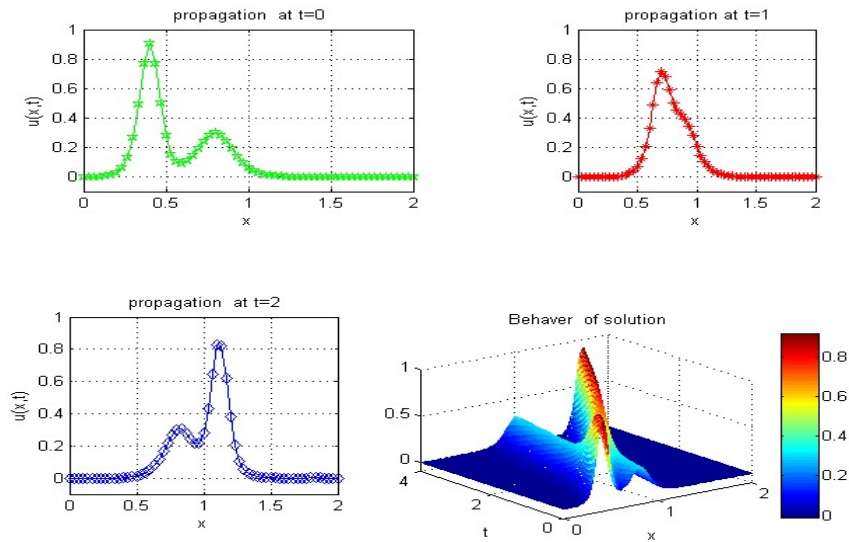| provided grid	points	estimated error at	provided grid point
x	t	L_∞	L_2
0.66667	3.9333	$4.7839E - 03$	$1.1526E - 04$
1.6667	3.9833	$4.4147E - 05$	$3.1165E - 06$
1.9667	3.9983	$3.5070E - 05$	$2.300E - 06$
2	4	$2.4568E - 06$	$2.300E - 06$

Figure 1: Graph of the physical behavior of the solution when $\beta = 4.25 \times 10^{-04}$ and $M = 61$ with high-frequency oscillations for Example 1 (A).

5 Discussions

In this paper, sixth-order compact finite difference method is presented for solving a one-dimensional KdV-Burger equation. At first stage, we discretized the solution interval for concerning spatial variable. Next by applying the Taylor series expansion, we discretization partial derivative of the model problem in (2) involving spatial variable, we obtain sixth-order finite difference

Table 2: Point-wise absolute error and root mean square error, for Example 1 (B) if $M = 61$

provided grid	points	estimated error at	provided grid point
x	t	L_∞	L_2
0.333	3.967	$4.7E-04$	$1.3838E-05$
0.8333	3.9917	$3.600E-05$	$32.2569E-06$
0.9833	3.9992	$3.532E-06$	$1.3216E-07$
1	4	$2.473E-07$	$3.2814E-08$

Table 3: Point-wise absolute error and root mean square error, for Example 1 (C) if $M = 61$

provided grid	points	estimated error at	provided grid point
x	t	L_∞	L_2
1.333	3.8667	$7.2E-04$	$3.6786E-05$
3.333	3.9677	$9.7E-05$	$4.0591E-06$
3.9333	3.9967	$6.25E-07$	$5.1082E-07$
4	4	$3.348E-07$	$3.126E-08$

Table 4: Point-wise absolute error and root mean square error obtained by the present method, for Example 2 using different step sizes h and time step

provided step size and	time step	Estimated Error at	provided grid point
h	$\triangle t$	L_∞	L_2
0.1	0.5	$8.128E-04$	$2.1526E-05$
0.05	0.5	$5.9148E-05$	$7.6374E-06$
0.02	0.1	$4.1139E-05$	$5.2931E-06$
0.01	0.1	$3.8425E-06$	$9.2631E-07$

Table 5: Point-wise absolute error and root mean square error obtained by the present method, for Example 3 with different step sizes h and time step

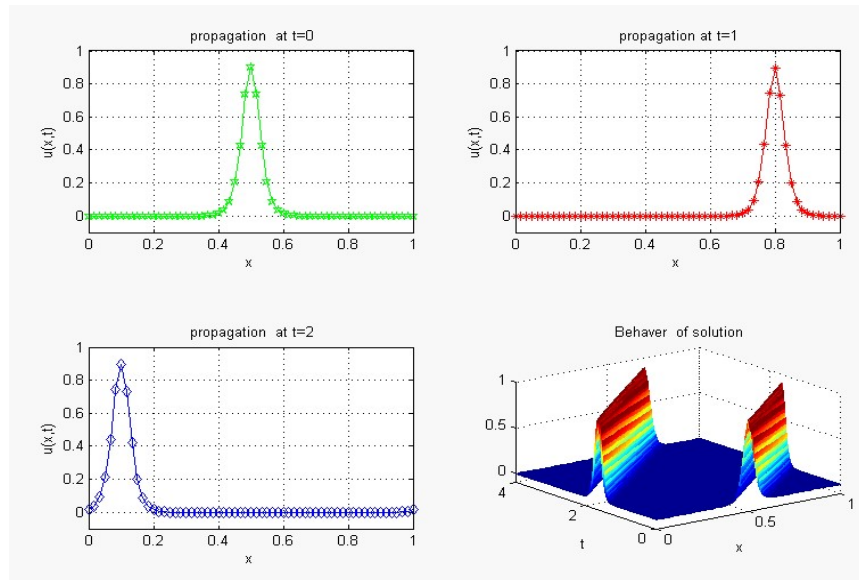| provided dance step size and	time step	Estimated Error at	provided grid point
h	$\triangle t$	L_∞	L_2
0.1	0.04	$1.3298E-06$	$6.3691E-07$
0.1	0.03	$5.1653E-07$	$4.6334E-07$
0.1	0.02	$4.623E-07$	$4.211E-07$
0.1	0.01	$1.975E-07$	$8.091E-08$

Figure 2: Graph of the physical behavior of the solution when $\beta = 4 \times 10^{-04}$ and $M = 61$ with high-frequency oscillations for Example 1 (B).
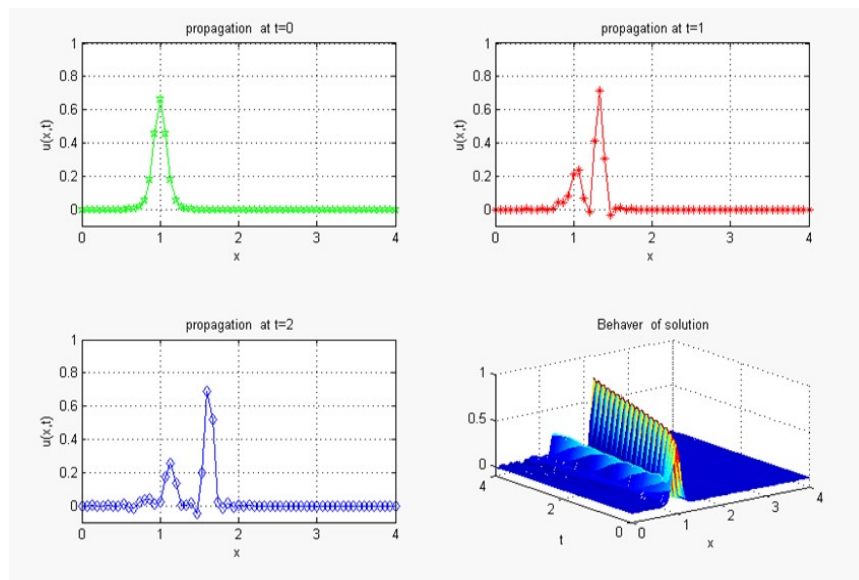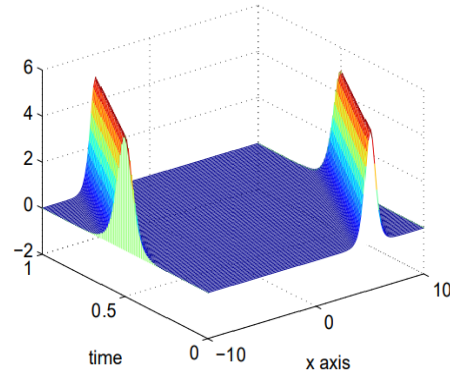

Figure 3: Graph of the physical behavior of the solution when $\beta = 10^{-04}$ and $M = 61$ with high-frequency oscillations for Example 1 (C).

a) Surface of exact solution
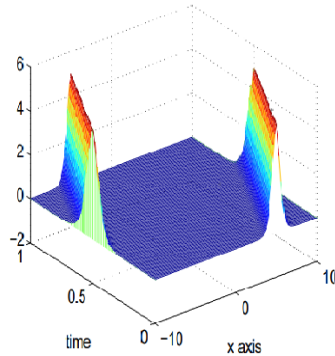

b) Above-ground of approximation result

Figure 4: Graph of the physical behavior of the surface of the present numerical solution with mesh sizes $h = 0.01$ and $k = 0.01$ for Example 2 which we compare it with the surface of exact solution in [37]

scheme. Then, by rearranging these semi-discretized schemes and combining them into the remaining part of partial derivative in the model problem concerning temporal variable without linearizing it. We obtain a system of nonlinear ODEs. Then, we solve the obtained system by using the fourth-order Runge–Kutta method. To demonstrate the competence of playacting (to identify the applicability and validity of the present proposed scheme), four model examples are solved by taking different values for step sizes h and dispersion coefficients v, α, and β in the different solution domains. To further verify this validity of the proposed method, the norm of errors between the numerical results for model problem in Example 1 subjected to three different initial conditions associated with numerical results obtained by dabbling mesh size $(2M, 2N)$ taking as the exact solution, is summarized
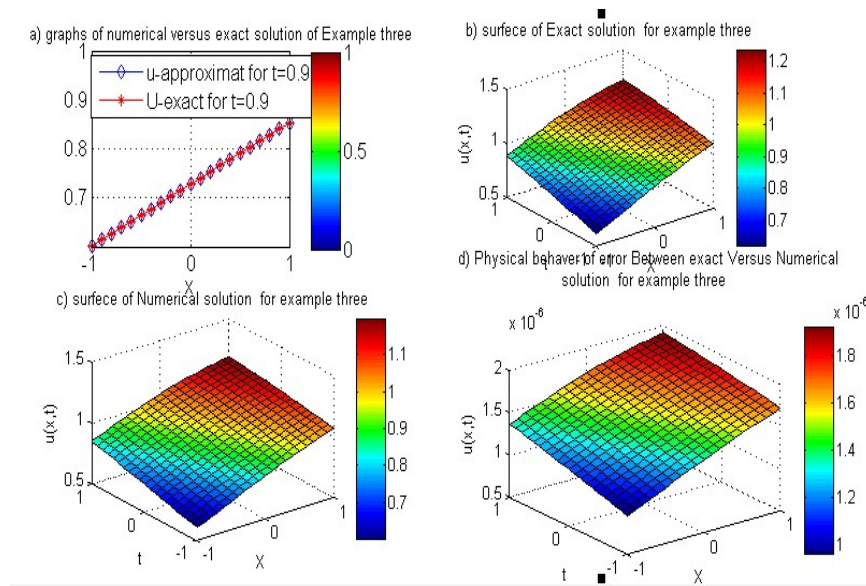
Figure 5: Graph of the physical behavior of the surface of the present numerical solution with mesh sizes $h = 0.05$ and $k = 0.01$ for Example 3, which we compare it with the solution in [30]

Table 6: Comparison of point-wise absolute error and root mean square error, for Example 4 using different step sizes h and time step $\triangle t$

provided step size and time step			
result by present method		Estimated Error at	provided grid point
h	$\triangle t$	L_∞	L_2
1/10	1/20	$4.5349E - 05$	$8.3691E - 06$
1/30	1/20	$5.1653E - 06$	$5.6334E - 06$
1/50	1/20	$3.5283E - 06$	$9.4184E - 07$
Result by Method in [1]			
1/10	1/20	$1.5678E - 04$	$6.1032E - 04$
1/30	1/20	$7.8531E - 05$	$3.9868E - 05$
1/50	1/20	$1.6579E - 05$	$7.1991E - 06$

in Tables 1–3 and Figures 1–3 for different disparate parameters and its solution domain.

As it can be seen from these tables, the point-wise maximum absolute errors (L_∞) and root mean square error (L_2) are rapidly decreases as the value of x and t increase. This indicates that the vibration of the solution line has to become overlapping and that the dispersion of the travelling wave is equal. From those figures, also we can understand that, for different values of β and initial conditions, we obtain differences in diametrical travelling
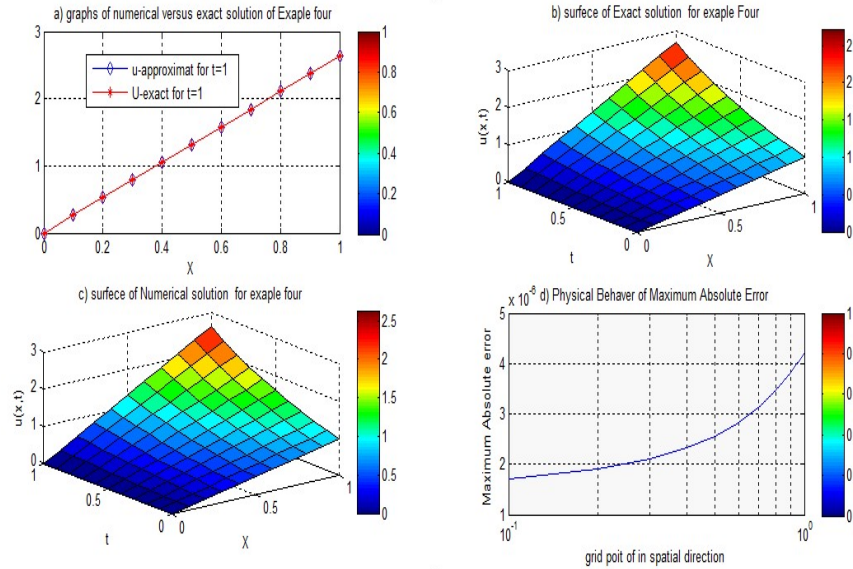
Figure 6: Graph of the physical behavior and surface of the present numerical solution with mesh sizes $h = 0.01$ and $\triangle t = 0.1$ for Example 4, which we compare it with the surface of exact solution in [1]

wave, and at a certain point in the assorted domain, the vibration line of the travelling wave is overlapping. Hence, in this case, a numerical approximation of Example 1 for different values of β, initial conditions, and the solution interval is very well, and it gives different behaviors of the solution. From Table 4 and Figure 4, we conclude that the present numerical resolution for Example 2 is accurate than the quantitative result in [37]. Thus this not only shows the solution given by the graphical form, but also as we saw from Table 4, if mesh-size decreases, both roots mean square error and point-wise error of the present numerical result are rapidly decreased. So that, this shows that the accuracy of the present acting method is increased and proves the preexisting accuracy. Hence the approximate solution by the present method for Example 2 is very well. Also, as we saw from Table 5 and Figure 5 that the present numerical solution of Example 3 is accurate than the numeric resolution in [30]. Because of, as it can be seen from the obtained error norm of numerical results specified in Table 5, both roots mean square error and maximum point-wise error are decreased. This shows the correcting and proving the preexisting results in [30]. Hence our result is more accurate than the event that exists in the literature. In addition to this, the present techniques are also used to solve a fractional order KdV-Burger equation. As it can be seen from the comparison of accuracy through the error norm for numerical results given in Table 6, the quality of the present method is more

superstar than the truth of solution in [1] for $\alpha = 0.9$. Because of both L_∞ and L_2 rapidly decrease as h decreases to zero with a fixed time step $\triangle t$.

Therefore, depending on all accuracy of the present numerical results, the proposed method validates and improves the accuracy of preexisting methods described in the literature. Also in this paper, both the theoretical and numerical error bounds have been established. The obtained quantitative results listed in the tables and graphs are also confirmed our established computational rate of convergence and theoretical estimates of the error bound.

6 Conclusion

In this study, a new approach, which was called sixth-order compact finite difference method, was presented to solve a one-dimensional KdV-Burger equation. The comparison of results obtained by the present method acting was more convenient, reliable, and effective than some methods listed in the literature. An error analysis based on the von Neumann stability investigating was also developed for the present study. So that, as it can be seen from both graphs and tables, the accuracy of the present method has improved the inaccuracy of preexisting techniques in literature by decreasing the value of h and $\triangle t$. As a summary, the accuracy of numerical results given in terms of tables and graphs indicated that as the values of h and $\triangle t$ decrease, the errors drop-off more rapidly. Generally, this technique is a reliable acting method and ables solving the one-dimensional KdV-Burger equation. Based on the findings, this method is well approximate and gives better accuracy of the numerical solution with both decreasing or some fixed step sizes h and time step $\triangle t$. Therefore this method is a suitable technique to approximate the exact solution of PDE very well.

Acknowledgments

References

1. Ahmad, I., Ahmad, H., Inc, M., Rezazadeh, H., Akbar, M.A., Khater, M.M., Akinyemi, L. and Jhangeer, A. *Solution of fractional-order Korteweg-de Vries and Burgers' equations utilizing local meshless method*, J. Ocean Eng. Sci. (2021).

2. Ahmad, H., Khan, T.A., Stanimirovic, P.S. and Ahmad, I. *Modified variational iteration technique for the numerical solution of fifth order KdV-*

type equations, J. Appl. Comput. Mech. (2020).

3. Aliyi, K. and Muleta, H. *Numerical method of the line for solving one dimensional initial-boundary singularly perturbed Burger equation*, Indian J. Adv. Math. 1(2) (2021), 4–14.

4. Aliyi, K., Shiferaw, A. and Muleta, H. *Radial basis functions based differential quadrature method for one dimensional heat equation,* American Journal of Mathematical and Computer Modelling, 6 (2021), 35–42.

5. Benney, D.J. *Long waves on liquid films*, J. Math. Phys. 45 (1966), 150–155.

6. Chen, B. and Xie, Y.C. *Exact solutions for wick-type stochastic coupled Kadomtsev- Petviashili equations,* J. Phys. A, 38 (2005), 815–822.

7. Chen, B. and Xie, Y.C. *Exact solutions for generalized stochastic Wick-type KdV-mKdV equations* , Chaos Solitons Fractals, 23 (2005), 281–287.

8. Chen, B. and Xie, Y.C. *Periodic-like solutions of variable coefficient and Wick type stochastic NLS equations*, J. Comput. Appl. Math. 203 (2007), 249–263.

9. Feng, Z. and Qing-guo, M. *Burgers-Korteweg-de Vries equation and its travelling solitary waves* , Sci. China Ser. A, 50 (3) (2007), 412-422.

10. Gao, G. *A theory of interaction between dissipation and dispersion of turbulence* , Sci. Sinica Ser. A, 28 (1985), 616–627.

11. Ghany, H.A., and Fathallah, A. *Exact solutions for KDV-Burger equations with an application of white-noise analysis* , Int. J. Pure Appl. Math. 78(1) (2012), 17–27.

12. Gowrisankar, S. and Natesan, S. *Uniformly convergent numerical method for singularly perturbed parabolic initial-boundary-value problems with equidistributed grids,* Int. J. Comput. Math. 91 (2014), 553–577.

13. Grad, H. and Hu, P.N. *Unified shock profile in a plasma*, Phys Fluids, 10 (1967), 2596–2602.

14. Gurlu, Y.U. and Kaya, D. *Analytic method for solitary solutions of some partial differential equations*, Phys. Lett. A, 370 (2007), 251–259.

15. Hixon, R. and Turkel, E. *Compact implicit MacCormack-type schemes with high accuracy*, J. Comput. Phys. 158 (2000), 51–70.

16. Hu, P.N. *Collisional theory of shock and nonlinear waves in a plasma.* , Phys. Fluids. 15 (1972), 854–864.

17. Johnson, R.S. *A nonlinear equation incorporating damping and dispersion* , J. Fluid Mech. 42 (1970), 49–60.

18. Johnson, R.S. *Application of He's homotopy perturbation method to non-linear integro-differential equations*, Appl. Math. Comput. 188(1) (2007), 538–548.

19. Johnson, R.S. *A modern introduction to the mathematical theory of water waves,* Cambridge, Cambridge University Press, 1997.

20. Kashchenko, S.A. *Normal form for the KdV-Burgers equation*, Dokl. Math. 93 (2016), 331–333.

21. Kaya, D. *An application of the decomposition method for the two-dimensional KdV-Burgers equation* , Comput. Math. Appl. 48 (2004), 1659–1665.

22. Koroche, A. K. *Numerical solution for one dimensional linear types of parabolic partial differential equation and application to heat equation*, Mathematics and Computer Science, 5 (2020), 76–85.

23. Korteweg, D.J. and de Vries, G. *On the change of form of long waves advancing in a Rectangular canal and on a new type of long stationary waves*, Lond. Edinb. Dublin philos. mag. j. sci. 39 (1895), 22–43.

24. Kudryashov, N.A. *On "new travelling wave solutions" of the KdV and the KdV-Burgers equations,* Commun. Nonlinear Sci. Numer. Simul. 14(5) (2009), 1891–1900.

25. Kutluay, S., Esen, A. and Dag, I. *Numerical solutions of the Burgers' equation by the least-squares quadratic B-spline finite element method*, J. Comput. Appl. Math. 167 (2004), 21–33.

26. Li, J. and Visbal, M.R. *High-order compact schemes for nonlinear dispersive waves*, J. Sci. Comput., 26 (2006), 1–23.

27. Navon, I.M. and Riphagen, H.A. *An implicit compact fourth order algorithm for solving the shallow-water equations in conservation-law form* , Mon. Weather Rev. 107 (1979), 1107–1127.

28. Navon, I.M. and Riphagen, H.A. *SHALL4 – An implicit compact fourth-order Fortran program for solving the shallow-water equations in conservation-law form* , Comput. Geosci. 12 (1986), 129–150.

29. Shang, J.S. *High-order compact-difference schemes for time-dependent Maxwell equations*, J. Comp. Phys. 153 (1999), 312–333.

30. Shi, Y.F. , Xu, B. and Guo, Y. *Numerical solution of Korteweg-de Vries-Burgers equation by the compact-type CIP method*, Adv. Differ. Equ. (2015), 1–9.

31. Spotz, W.F. and Carey, G.F. *Extension of high order compact schemes to time dependent problems* , Numer. Methods Partial Differential Equations 17 (2001), 657–672.

32. Visbal, M.R. and Gaitonde, D.V. *Very high-order spatially implicit schemes for computational acoustics on curvilinear meshes,* J. Comput. Acoust. 9 (2001), 1259–1286.

33. Wadati, M. *Deformation of solitons in random media*, J. Phys. Soc. Japan 59 59 (1990), 4201–4203.

34. Wadati, M. and Akutsu, Y. *Stochastic Korteweg de Vries equation,* J. Phys. Soc. Japan, 53 (1984), 3342–3350.

35. Wazzan, L. *A modified tanh-coth method for solving the KdV and the KdV–Burgers equations* , Commun. Nonlinear Sci. Numer. Simul. 14 (2009), 443–450.

36. van Wijngaarden, L. *On the motion of gas bubbles in a perfect fluid* , Arch. Mech. (Arch. Mech. Stos.) 34(3) (1982), 343–349 (1983).

37. Xiang, T. *A summary of the Korteweg-de Vries Equation*, (2015).

38. Xie, Y.C. *Exact solutions for stochastic KdV equations*, Phys. Lett. A, 310 (2003), 161–167.

How to cite this article